Nuclear Magnetic Resonance for characterization of atomic arrangements in real structures of intermetallic compounds

Matej Bobnar[#], Alfred Amon, Michael Baitinger, Bodo Böhme, Xianjuan Feng, Andreas Leithe-Jasper, Ulrich Schwarz, Igor Veremchuk, Xinke Wang, Yuri Grin

In Nuclear Magnetic Resonance (NMR) spectroscopy, each individual nucleus possessing a magnetic moment can produce a resonant signal at a specific frequency depending on its local magnetic field. Thus, in a sample containing many nuclei, the NMR spectrum is a distribution of signals from individual nuclei, which makes NMR a suitable method for studies of local atomic environments. This can be contrasted to the X-ray methods, for which an ensemble of atoms is responsible for producing a signal, elucidating only the average structure.

Studies of disorder

As a local probe, NMR is a suitable method for studies of local disorder. An extreme case of a locally disordered system is an amorphous material. Recently, we synthesized an amorphous phase with the approximate composition Zn_2Si_5(:H, OH) by heterogeneous oxidation of Li_2ZnSi with the ionic liquid DTAC-$AlCl_3$ [1]. The surface of the binary bulk Zn_2Si_5 features Si–H and Si–OH terminations (see report Böhme).

The ^{29}Si signal of the synthesized multicomponent product covered shift ranges from 80 ppm to -180 ppm. However, the ^{1}H-^{29}Si cross-polarization (CP) experiments showed that almost all Si atoms with close distances to the H atoms have chemical shifts in the range of $SiO_{4-x}(OH)_x$ or Si–H species (-40 ppm to -110 ppm). Therefore, the strong signal contributions in the ^{29}Si echo spectra around 0 ppm and below arise from an oxygen-free phase, in which Si atoms have large distances to hydrogen atoms. We therefore assigned this signal contribution to Si atoms of a bulk amorphous phase, in which the Si atoms form bonds to Si and to Zn, rather than to hydrogen atoms.

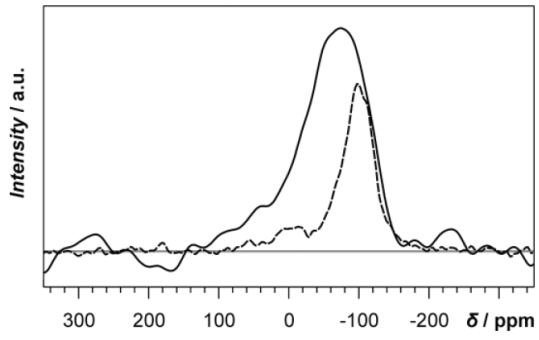

Fig.-1: ^{29}Si Magic Angle Spinning (MAS) NMR spectra of Zn_2Si_5(:H, OH): Solid curve represents an echo spectrum, dashed curve a ^{1}H-^{29}Si CP spectrum, normalized to 75% of the maximum intensity of the echo spectrum.

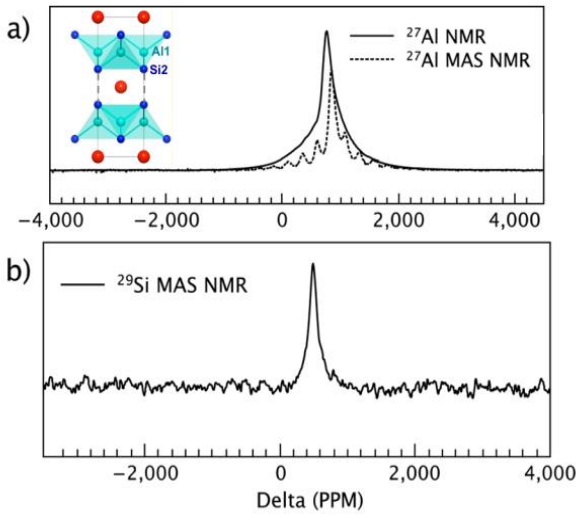

Fig.-2: (a) ^{27}Al NMR spectrum and the crystal structure of tI10-$SrAl_2Si_2$. The solid line represents the static frequency-swept spectrum and the dotted curve shows the spectrum obtained via MAS. (b) ^{29}Si NMR MAS spectrum of tI10-$SrAl_2Si_2$.

Possible site disorder was investigated in metastable *tI*10-$SrAl_{4-x}Si_x$ materials ($0 \le x \le 2$) [2], a high-pressure modification of the ambient-pressure compound *hP*5-$SrAl_2Si_2$. The high-pressure compound *tI*10-$SrAl_2Si_2$, crystallizing in a $BaZn_2P_2$ structure type, has two crystallographic positions (4*d* and 4*e*), in which Si or Al can reside (see report Schwarz).

Due to the similar atomic scattering factors of Si and Al, their site preference could not be determined by X-ray diffraction. However, the ^{27}Al MAS results suggest that the Al signal arises primarily from a single crystallographic position. Nevertheless, the absence of a distinctively shaped satellite background in the static spectrum (like it can be observed for both Al positions in $SrAl_4$) points to the fact that some disorder in the site occupancy remains. Likewise, ^{29}Si MAS NMR spectroscopy also showed only one signal, an indication of a single Si position. A conclusive

indication that Si occupies site 4*e* was attained with the help of DFT calculations and by making use of the fact that the more electronegative elements in this structure type preferentially occupy site 4*e*.

Detection of X-ray-poorly-scattering nuclei

The atomic scattering of the X-ray diffraction increases with increasing atomic number. This makes detection and structure refinement of the light atoms very difficult, particularly when compounds are made up of both heavy and light elements. In these cases, NMR can often help elucidating the structure, since most light elements have isotopes of very high sensitivity in NMR, such as ^{1}H, ^{6,7}Li, ^{9}Be, ^{11}B, ^{13}C,…

We succeeded in a preparation of the first ternary lithium-silicon clathrate $[Li_xBa_{8-x}][Si_{46-y}Li_y]$ with Li atoms substituting Ba in the cages as well as Si in the framework [3] (see report Baitinger). The ^{7}Li-NMR spectrum of the Li-containing clathrate phase (Fig.3, top) showed two weak signals. The signal at around 300 ppm was assigned to Li replacing Ba in the cages. An assignment of the signal at 0 ppm to the Li framework atoms, however, was not unambiguous, because contributions of Li-containing oxidic by-products from the washing process were conceivable. The sole ^{7}Li-NMR signal at 0 ppm of the precursor clathrate phase $Ba_{8-x}Si_{46}$ (Fig.3, bottom) was very weak, confirming that the clathrate phase contained practically no lithium. Also in this case, the signal might have originated from contaminants. However, after reacting the initial clathrate phase with the precursor phase $Ba_4Li_2Si_6$, two distinct signals were detected (Fig.3 middle), providing evidence that Li was incorporated into the clathrate phases.

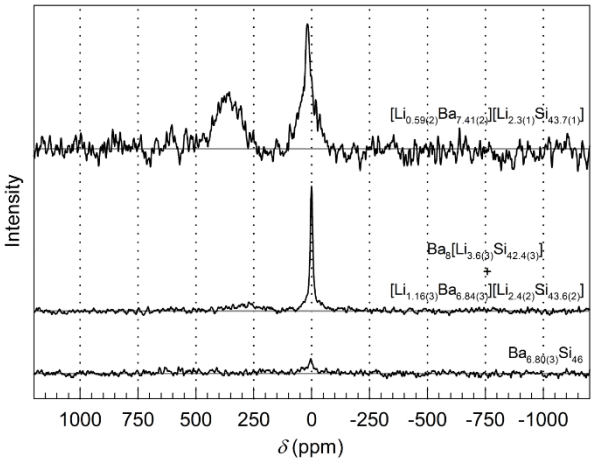

Fig.-3: ^{7}Li-NMR spectra of different clathrate products.

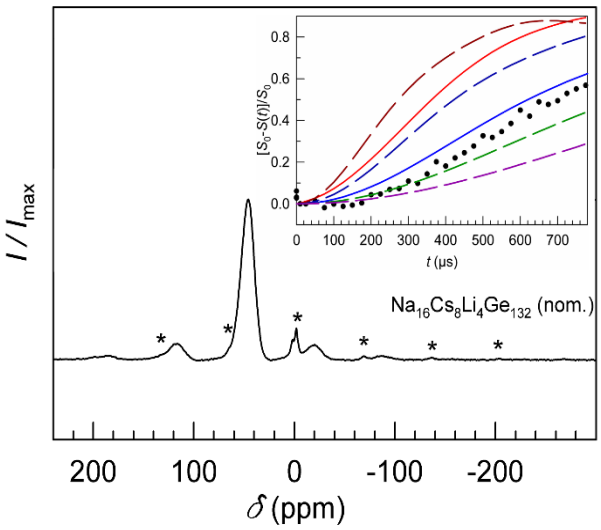

Fig.-4: ^{7}Li MAS NMR spectrum of the sample with the nominal composition $Na_{16}Cs_8Li_4Ge_{132}$. Asterisks mark the central transition ($\delta \approx 0$) and rotational side bands of a contaminant. Inset: The results of the SEDOR experiment (dots) with simulated curves for different models.

Subsequently, the intermetallic type-II clathrate phase $Na_{16}Cs_8Li_xGe_{136-x}$ with composition $x \approx 2.8$ and Li substituting Ge atoms in the framework was prepared [4]. The phase composition was established by crystal structure refinement and was supported by microstructure and chemical analyses as well as NMR. ^{7}Li NMR of the clathrate phase revealed a signal at 45 ppm with the corresponding sidebands. The considerable Knight shifts of the ^{7}Li, ^{23}Na, and ^{133}Cs signals point to the metallic property of the clathrate. The fixed-time Spin Echo Double Resonance (SEDOR) experiment was employed to confirm the incorporation of the Li into the bulk clathrate phase. Comparing the measured SEDOR ratio and the simulated curves showed that the distance between Li and Cs atoms from the clathrate cages cannot be larger than 5 Å. Thus, some sites of the crystal structure could be ruled out as possibilities for an occupation by Li (see report Baitinger).

Detection of dopants

Another hardship for many methods is the detection and characterization of dopant atoms. In such cases, NMR is useful if doping atoms have a sufficient NMR sensitivity and the conditions are right. For example, metallic and paramagnetic samples allow for rapid collection of the signal, and with sufficient time and dopant concentration a signal can be observed.

Recently, we studied Na-doped PbTe, a known thermoelectric material [5]. Two different substitution schemes, $Pb_{1-x}Na_xTe$ and $Pb_{1-y}Na_yTe_{1-y/2}$, were systemically investigated, and different solubility ranges for each series were established: 1.0 at. % for $Pb_{1-x}Na_xTe$, and 2.5 at. % for $Pb_{1-y}Na_yTe_{1-y/2}$. ^{23}Na NMR revealed two main peaks of interest, which appeared with different magnitude according to the preparation and treatment of the samples. The first signal at around -14 ppm was assigned to Na replacing Pb in the crystal structure; it was the main signal of all $Pb_{0.98}Na_{0.02}Te$ samples as well as the $Pb_{0.95}Na_{0.05}Te_{0.975}$ sample after annealing. The signal at 40.7 ppm was assigned to Na replacing Pb near a Te vacancy. A similar chemical shift was found for the binary Na_2Te, where Na is fourfold coordinated by Te. The larger shift and the large relative intensity of the signal at 40.7 ppm can be understood by assuming a clustering of the Na atoms around the Te defect in order to reduce the local excess charge appearing by the vacancy formation (see report Veremchuk).

A long standing question of Al incorporation into the heavy fermion superconductor UBe_{13} was investigated in an effort to explain a sample dependence of physical properties [6]. The substitution of Be by 1 - 2 at. % Al resulted in the increase of the lattice parameter and the

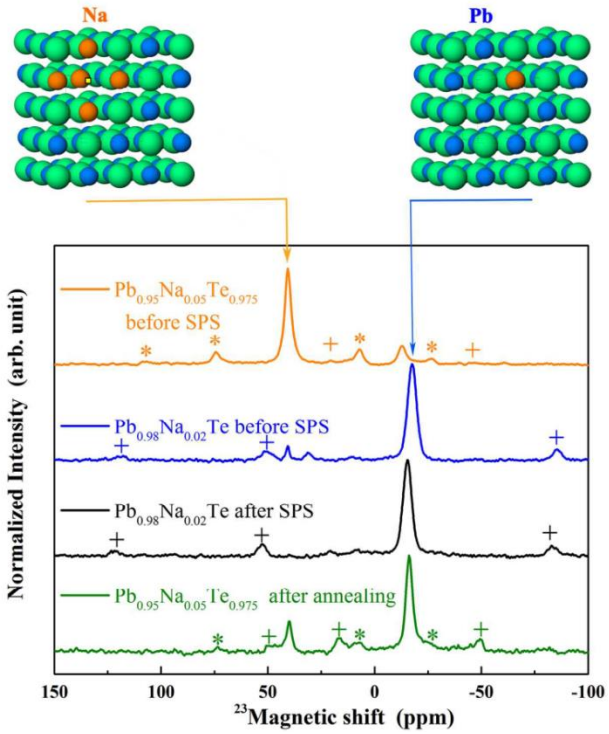

Fig.-5: ^{23}Na MAS NMR spectra of PbTe substituted with Na. Spinning sidebands from the left and right signals are marked by asterisks and crosses, respectively.

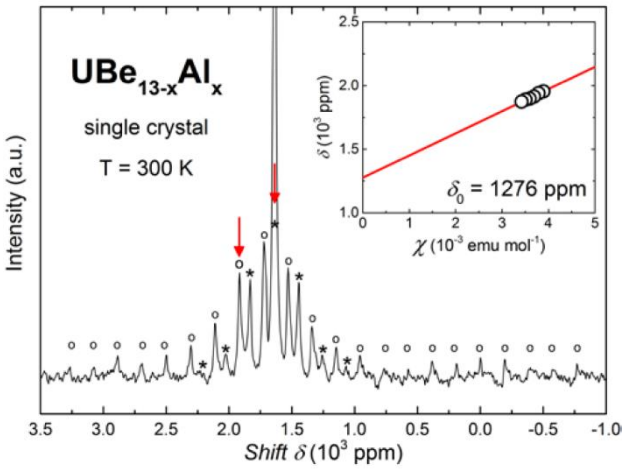

Fig.-6: ^{27}Al MAS NMR spectra of a powdered single-crystal of $UBe_{13-x}Al_x$. Signals for Al incorporated in $UBe_{13-x}Al_x$ (central line δ = 1915 ppm, circles) and Al flux residue (δ = 1635 ppm, asterisks) are indicated by arrows. Inset: Al-signal shift in $UBe_{13-x}Al_x$, as a function of temperature-dependent magnetic susceptibility.

concomitant change of the superconducting properties. Evidence for incorporated Al in flux-grown UBe_{13} single crystals was obtained by X-ray diffraction and spectroscopy, atomic resolution transmission electron microscopy, and NMR. ^{27}Al MAS NMR spectroscopy on powdered single crystals of $UBe_{13-x}Al_x$ revealed two sharp, strongly overlapping signals (Fig. 6). The signal with an isotropic Knight shift δ = 1915 ppm originates from Al incorporated in $UBe_{13-x}Al_x$. At particular temperatures, it overlaps with a strong signal from the Al metal flux residue (δ = 1635 ppm). The temperature dependence of the signal at δ = 1915 ppm is consistent with paramagnetism in UBe_{13} (inset of Fig. 6). Furthermore, pulse length optimization for this signal revealed that about 2 to 3 times shorter pulses are required for maximum intensity compared to the signal of pure Al metal. This indicates non-zero quadrupolar coupling, which is a sign of non-cubic site symmetry for Al in $UBe_{13-x}Al_x$, thus excluding substitution on the Be1 site at the icosahedron center (see report Svanidze).

Summary & Outlook

As a local probe, we used NMR to study disorder in crystalline as well as amorphous materials. Furthermore, employing NMR was a practical way of locating atoms that are difficult to detect by e.g. X-ray methods, in particular such nuclei with small atomic number. Finally, we used NMR to detect whether doping elements are incorporated into the main phase.

There are many more materials that we wish to investigate in this respect, be it compounds related to the ones that we have recently studied or other, hitherto not investigated classes of materials. Moreover, we want to extend NMR to the area of the physics and dynamics of the studied materials. At present, NMR spectroscopy is - within the department of Chemical Metals Science - perhaps not a standard investigation method, however, it is irreplaceable for the solution of particular problems.

External Cooperation Partners

A. Zevalkink (MSU, Lansing, MI, USA); K. Wei, G. S. Nolas (USF, Tampa, FL, USA)

References

[1] *An Amorphous Phase of Zinc and Silicon at Composition Zn_2Si_5(:H, OH), X.-J. Feng, B. Böhme, M. Bobnar, P. Simon, W. Carrillo-Cabrera, U. Burkhardt, M. Schmidt, U. Schwarz, M. Baitinger, T. Strassner and Y. Grin, Zeitschrift für anorganische und allgemeine Chemie **643**, (2017) 106, doi.org/10.1002/zaac.201600340.*

[2] *Making and Breaking Bonds in Superconducting $SrAl_{4-x}Si_x$ (0 <= x <= 2). A. Zevalkink, M. Bobnar, U. Schwarz and Y. Grin, Chemistry of Materials **29**(3) (2017) 1236, doi.org/10.1021/acs.chemmater.6b04615.*

[3] *Type-I silicon clathrates containing lithium, B. Böhme, M. Bobnar, A. Ormeci, S. Peters, W. Schnelle, M. Baitinger and Y. Grin, Zeitschrift für Kristallographie **232**(1-3), (2017) 223, doi:10.1515/zkri-2016-1983.*

[4] *A type-II clathrate with a Li-Ge framework, B. Böhme, K. Wei, M. Bobnar, Y. Prots, U. Burkhardt, M. Baitinger, G. S. Nolas and Y. Grin, Zeitschrift für Kristallographie **232**(7-9) (2017) 543, doi.org/10.1515/zkri-2017-2046.*

[5] *Sodium Substitution in Lead Telluride, X. Wang, I. Veremchuk, M. Bobnar, U. Burkhardt, J.-T. Zhao and Y. Grin, Chemistry of Materials **30**(4) (2018) 1362, doi.org/10.1021/acs.chemmater.7b05091.*

[6] *Tracking aluminum impurities in single crystals of the heavy-fermion superconductor UBe_{13}, A. Amon, I. Zelenina, P. Simon, M. Bobnar, M. Naumann, E. Svanidze, F. Arnold, H. Borrmann, U. Burkhardt, W. Schnelle, E. Hassinger, A. Leithe-Jasper and Y. Grin, Sci. Rep.**8** (2018) 10654.*

[#] Matej.Bobnar@cpfs.mpg.de